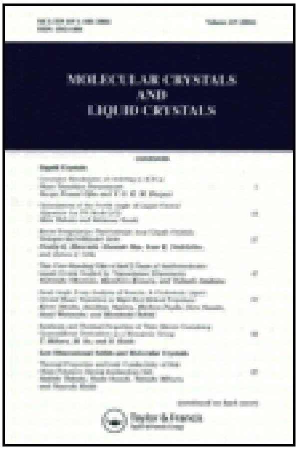

Molecular Crystals and Liquid Crystals
Publication details, including instructions for authors and subscription information:
http://www.tandfonline.com/loi/gmcl20

Efficiency Stabilization in Blue Organic Light-Emitting Devices Fabricated Utilizing a Double Emitting Layer with Fluorescence and Phosphorescence Doped Layers

H. S. Bang [a], D. C. Choo [a], T. W. Kim [a], J. H. Park [b], J. H. Seo [b] & Y. K. Kim [b]

[a] Research Institute of Information Display, Division of Electronics and Computer Engineering, Hanyang University, Seongdong-gu, Seoul, Korea

[b] Department of Information Display Engineering & Center for Organic Materials & Information Display (COMID), Hong-ik University, Seoul, Korea

Version of record first published: 22 Jul 2010

Mol. Cryst. Liq. Cryst., Vol. 498, pp. 265–273, 2009

ISSN: 1542-1406 print/1563-5287 online
DOI: 10.1080/15421400802619388

Efficiency Stabilization in Blue Organic Light-Emitting Devices Fabricated Utilizing a Double Emitting Layer with Fluorescence and Phosphorescence Doped Layers

H. S. Bang[1], D. C. Choo[1], T. W. Kim[1], J. H. Park[2], J. H. Seo[2], and Y. K. Kim[2]
[1]Research Institute of Information Display, Division of Electronics and Computer Engineering, Hanyang University, Seongdong-gu, Seoul, Korea
[2]Department of Information Display Engineering & Center for Organic Materials & Information Display (COMID), Hong-ik University, Seoul, Korea

The luminance efficiency of the blue organic light-emitting devices (OLEDs) fabricated utilizing a double emitting layer (DEML) with a 4,4′-Bis(2,2-diphenyl-ethen-1-yl)diphenyl (DPVBi) layer doped with 4,4′-Bis[4-(diphenylamino)styryl]biphenyl (BDAVBi) fluorescence dopant and a 4,4′-Bis(carbazol-9-yl)biphenyl (CBP) layer doped with a bis(3,5-difluoro-2-(2-pyridyl)phenyl-(2-carboxypyridyl)iridium III (FIrpic) phosphorescence dopant at 20 mA/cm^2 was 6.2 cd/A, indicative of highly efficient OLEDs. Electroluminescence spectra for the OLEDs with a DEML showed that a dominant peak at 469 nm corresponding to the BDAVBi doped DPVBi layer together with a shoulder at 491 nm related to the combination of the BDAVBi doped DPVBi layer and the FIrpic doped CBP layer appeared.

Keywords: blue emitting layer; efficiency stabilization; fluorescence; luminance efficiency; organic light-emitting devices; phosphorescence

INTRODUCTION

Organic light-emitting devices (OLEDs) have emerged as promising candidates for potential applications in the fabrication of highly-efficient

This work was supported by the Korea Science and Engineering Foundation (KOSEF) grant funded by the Korea government (MEST) (No. R0A-2007-000-20044-0)
Address correspondence to Prof. T. W. Kim, Research Institute of Information Display, Division of Electronics and Computer Engineering, Hanyang University, 17 Haengdang-dong, Seongdong-gu, Seoul 133–791, Korea (ROK). E-mail: twk@hanyang.ac.kr

full-color flat-panel displays [1–5]. OLED displays have attracted much attention due to their use in promising full color displays, which offer unique advantages of low driving voltage, low power consumption, high contrast, wide viewing angle, low cost, and fast response [6,7]. Potential applications of highly-efficient blue OLEDs have driven extensive efforts to fabricate various kinds of OLEDs with unique structures [8]. However, blue OLEDs still have inherent problems of low efficiency, poor color purity, and short lifetime in comparison with other red or green OLEDs [9]. Blue OLEDs with various structures were suggested for enhancing their efficiency and color stabilization [10–15]. Even though some works on the efficiency enhancement in green or white OLEDs fabricated utilizing a hole transport layer (HTL) with multiple heterostructures or with a double emitting layer (DEML) have been performed to improve the balance of holes and electrons in an emitting layer (EML) [16–21], studies concerning highly-efficient blue OLEDs fabricated utilizing a DEML with fluorescence and phosphorescence doped layers have not been reported yet because of the complicated device-fabrication process.

This paper reports the electrical and the optical properties of blue OLEDs fabricated with a DEML with fluorescence and phosphorescence doped layers deposited by using organic molecular-beam deposition (OMBD). Current density-voltage, luminance-voltage, and luminance efficiency-current density measurements were performed to investigate the electrical properties and the efficiency of the OLEDs fabricated utilizing a DEML with a 4,4′-Bis(carbazol-9-yl)biphenyl (CBP) layer doped with a 8% bis(3,5-difluoro-2-(2-pyridyl)phenyl-(2-carboxypyridyl)iridium III (FIrpic) dopant and a 4,4′-Bis(2,2-diphenyl-ethen-1-yl)diphenyl (DPVBi) layer doped with a 5% 4,4′-Bis[4-(diphenylamino)styryl]biphenyl (BDAVBi), respectively. Electroluminescence (EL) measurements were carried out to investigate the efficiency and the color stabilization of OLEDs with various kinds of structures. The Commission Internationale de l'Eclairage (CIE) chromaticity coordinates corresponding to the emission colors for OLEDs with various kinds of structures were investigated in order to clarify the blue color stabilization. The electrical and the optical properties of the OLEDs with a FIrpic doped CBP and a BDAVBi doped DPVBi DEML were compared with those of OLEDs with a FIrpic doped CBP EML or both a BDAVBi doped DPVBi and a FIrpic doped CBP step like EML.

EXPERIMENTAL DETAILS

The sheet resistivity and the thickness of the indium-tin-oxide (ITO) thin films coated on glass substrates used in this study were

15 Ω/square and 100 nm, respectively. The ITO coated substrates were cleaned using ultrasonication of acetone, methanol, then distilled water at 60°C for 15 min and were thoroughly rinsed in de-ionized water thoroughly. The chemically cleaned ITO substrates were kept for 48 h in isopropyl alcohol. After the chemically cleaned ITO substrates had been dried by using N_2 gas with a purity of 99.9999%, the surfaces of the ITO substrates were treated with an oxygen plasma for 2 min at an O_2 pressure of approximately 2×10^{-2} Torr. The three kinds of samples used in this study were deposited on ITO thin films coated on glass substrates by using OMBD with tungsten effusion cells and shutters at a chamber pressure of about 5×10^{-6} Torr and consisted of the following structures from the top: an aluminum (Al) (100 nm) cathode electrode, a lithium quinolate (Liq) (2 nm) electron injection layer (EIL), a tris(8-hydroxyquinolate) aluminum (Alq_3) (25 nm) electron transport layer (ETL), a 2,9-dimethyl-4,7-diphenyl-1,10-phenanthroline (BCP) (5 nm) hole blocking layer (HBL), three kinds of the EMLs, an N,N′-Bis(naphthalene-1-yl)-N,N′-bis(phenyl)-benzidine (NPB) (50 nm) HTL, an ITO anode electrode, and a glass substrate. The EMLs consisted of a 8% doped CBP layer (30 nm), a DEML consisting of a 5% BDAVBi doped DPVBi layer (15 nm) and a 8% FIrpic doped CBP layer (15 nm), or a DEML consisting of a 8% FIrpic doped CBP layer (15 nm) and a 5% BDAVBi doped DPVBi layer (15 nm). After organic and metal depositions, the OLED devices were encapsulated in a glove box with O_2 and H_2O concentrations below 1 ppm. A desiccant material consisting of a barium-oxide powder was used to absorb the residual moisture and oxygen in the encapsulated device. The Liq layer, acting as an EIL, leads to a lower turn-on voltage and higher power efficiency [13]. The deposition rates of the organic layers and the metal layers were approximately 0.1 and 0.15 nm/s, respectively, and the deposition rates were controlled by using a quartz crystal monitor. The size of the emitting region in the pixel was 3 mm × 3 mm. The current density – voltage characteristics of the OLEDs were measured on a programmable electrometer with built-in current and voltage measurement units (model SMU-236, Keithely). The luminance and color coordinates were measured by using a chromameter CS-100 A (Minolta), and the EL spectrum was measured by using a luminescence spectrometer LS50B (Perkin-Elmer).

RESULTS AND DISCUSSION

Figure 1 shows schematic diagrams of the fabricated blue OLEDs of devices (a) I, (b) II, and (c) III. The conventional phosphorescent blue

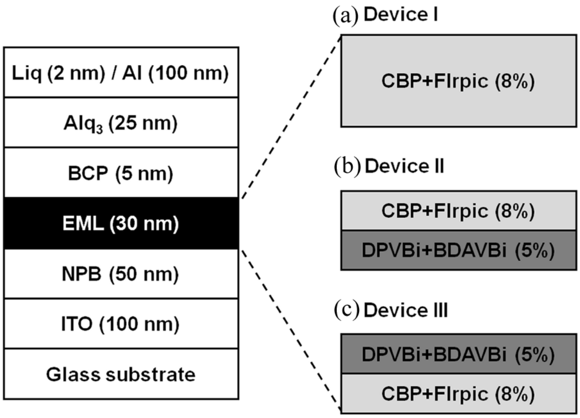

FIGURE 1 Schematic diagrams for the OLEDs of devices (a) I, (b) II, and (c) III.

OLED with a FIrpic-doped CBP EML is shown in Figure 1(a), and the blue OLEDs with a DEML consisting of a BDAVBi doped DPVBi layer and a FIrpic doped CBP layer or a DEML consisting of a FIrpic doped CBP and a BDAVBi doped DPVBi layer are shown in Figuress 1(b) and 1(c), respectively. The highest occupied molecular orbital (HOMO) and the lowest unoccupied molecular orbital (LUMO) levels of the NPB are −5.5 and −2.5 eV, respectively, as obtained from the cyclic voltametry [21], and the HOMO and the LUMO levels of the CBP layer are −6.3 and −3.2 eV, respectively [22]. The HOMO and the LUMO levels of the corresponding DPVBi layer are −5.9 and −2.8 eV, respectively [23], and the corresponding levels of the BCP layer are −6.7 and −3.2 eV, respectively [24]. The HOMO and LUMO levels of the corresponding FIrpic layer are −5.65 and 2.97 eV, respectively. The HOMO and LUMO levels of the corresponding BDAVBi layer are −5.34 and −2.63 eV, respectively [25].

Figure 2 shows (a) the current densities as functions of the applied voltage, (b) the luminances as functions of the applied voltage, and (c) the luminance efficiencies as functions of the current density for the OLEDs of devices I, II, and III. Filled squares, circles, and triangles represent the OLEDs of devices I, II, and III, respectively. The results of the current densities as functions of the voltage for all devices show almost similar behaviors. The LUMO level of the CBP single well is surrounded by the NPB and the BDAVBi doped DPVBi barriers, and the HOMO level of the BDAVBi doped DPVBi single well is surrounded by the FIrpic doped CBP EML and the BCP barriers. Since

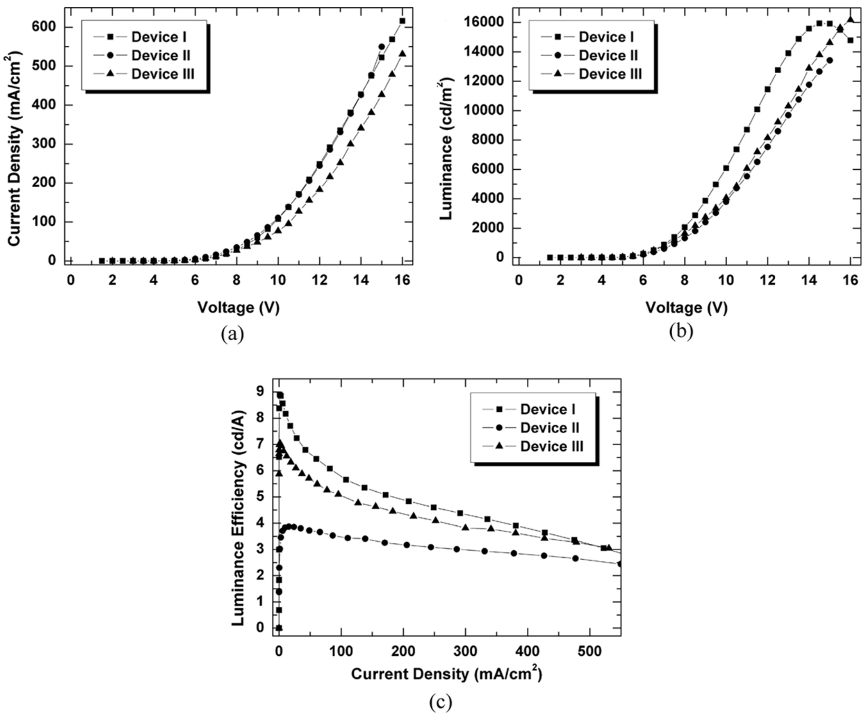

FIGURE 2 (a) Current densities as functions of the applied voltage, (b) luminance as functions of the applied voltage, and (c) luminance efficiencies as functions of the current density for OLEDs with various structures. Filled squares, circles, and triangles represent the OLEDs of devices I, II, and III, respectively.

the electrons are trapped and accumulated in the LUMO level of the FIrpic doped CBP single well in the OLEDs of a device III due to the existence in the barriers at the FIrpic doped CBP and the BDAVBi doped DPVBi heterointerfaces, the mobility of the holes in the single well, acting as an electron trapping layer, decreases, resulting in an enhancement in the efficiency of the OLEDs due to a better balance between the number of electrons and the number of holes. While the luminance of a device III at low voltage is lower than that of a device I, the corresponding luminance of device III is higher than that of a device II. However, the luminance of a device III above 15 V is higher than that of device I. Therefore, the enhanced luminance of device III in comparison with device I is attributed to the existence of the FIrpic doped CBP single well, resulting in a better balance between the holes and the electrons in the FIrpic doped CBP EML. Because the dominant EL peak for the OLEDs of devices II and III corresponds to a BDAVBi doped DPVBi layer in the DEML, the accumulated holes in the HOMO level of the BDAVBi doped DPVBi single well do not significantly affect the luminance of devices I, II, and III. The decrease in the luminance of a device III in comparison with that of a device I originates from going far away from the photopic vision curve or from the blue shift and the almost same value of full width at half maximum (FWHM) of the EL spectrum for a device I, which will be shown in Figure 3. While the luminance efficiency of a device I is the highest among the devices, the efficiency of a device I dramatically decreases with increasing current density. The decrease rates in the luminance efficiencies in the OLEDs of devices II and III are smaller than that of a device I, indicating that the efficiency stabilities of devices II and III are better than that of a device I.

Figure 3 shows the EL spectra at 10 V for devices I, II, and III. The dominant peaks of devices I, II, and III appear at 473, 469, and 469 nm, respectively, and the corresponding FWHMs are 49, 53, and

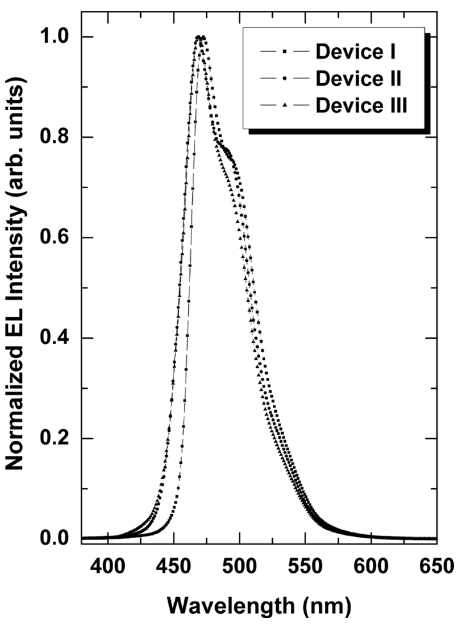

FIGURE 3 Electroluminescence spectra at 10 V for OLEDs with various structures. Filled squares, circles, and triangles represent the OLEDs of devices I, II, and III, respectively.

50 nm, respectively. The shoulder peaks of devices I, II, and III appear at 491 nm. The dominant peaks corresponding to the BDAVBi doped DPVBi layer in devices II and III shift to higher energy in comparison with that in a device I. The blue shift of the dominant peaks in devices II and III in comparison with a device I is attributed to the existence of the BDAVBi doped DPVBi layer, which is related to larger blue emission. After the holes accumulated at the NPB/CBP heterointerface for the OLEDs of device III are recombined with the electrons trapped in the NPB/FIrpic doped CBP/BDAVBi doped DPVBi single-well layer, the residual holes trapped in the FIrpic doped CBP/BDAVBi doped DPVBi/BCP single-well layer capture the electrons, which inject from the Alq_3 ETL into the CBP layer, resulting in the appearance of an EL peak at 469 nm due to a combination of the dominant peak corresponding to the BDABVi doped DPVBi layer and the shoulder peak corresponding to the FIrpic doped CBP layer.

Figure 4 shows CIE coordinates at 10 V for OLEDs of devices I, II, and III. The CIE coordinates of devices I, II, and III are (0.175, 0.355), (0.168, 0.297), and (0.167, 0.314), respectively. Since the blue

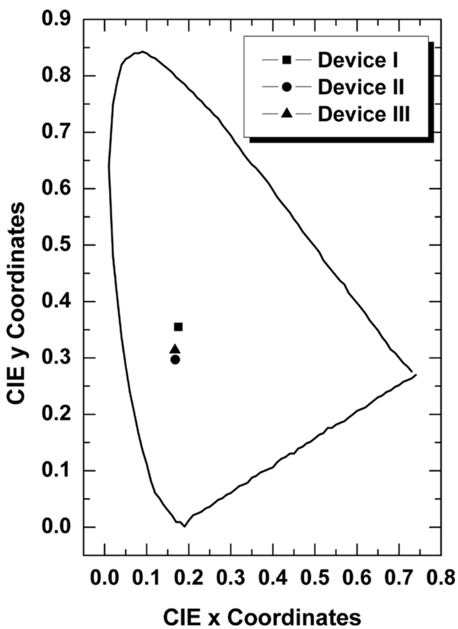

FIGURE 4 Commission Internationale de l'Eclairage (CIE) coordinates at 10 V for the OLEDs with various structures. Filled squares, circles, and triangles represent the OLEDs of devices I, II, and III, respectively.

portion of the emission spectrum for OLEDs with a BDAVBi doped DPVBi layer is deeper than that for OLEDs with a FIrpic doped CBP layer, the emission region of the OLEDs with a DEML consisting of a BDAVBi doped DPVBi layer and a FIrpic doped CBP layer is localized at the BDAVBi dope DPVBi layer. Furthermore, since the emission intensity corresponding to the shoulder peak at the BDAVBi doped DPVBi single-well layer in the DEML heterointerface between the FIrpic doped CBP layer and the BDAVBi doped DPVBi layer is lower, the color stability of a device III with a DEML becomes enhanced.

SUMMARY AND CONCLUSIONS

The electrical and the optical properties of blue OLEDs with a FIrpic doped CBP/BDAVBi doped DPVBi DEML consisting of fluorescence and phosphorescence layers were investigated. The luminance efficiency of the OLEDs with a DEML was stabilized for the variation of the current density. The dominant peak corresponding to the BDAVBi doped DPVBi layer for the electroluminescence spectrum in the OLEDs with a DEML appeared at 469 nm, and the shoulder peak related to the FIrpic doped CBP layer appeared at 491 nm. The CIE coordinates of the OLEDs with a DEML at 10 V were (0.167, 0.314), indicative of a stabilized blue color. These results indicate that efficiency stabilized blue OLEDs can be fabricated utilizing a DEML consisting of fluorescence and phosphorescence doped layers.

REFERENCES

[1] Tang, C. W. & Van Slyke, S. A. (1987). *Appl. Phys. Lett.*, *51*, 913.
[2] Baldo, M. A., O'Brien, D. F., You, Y., Shoustikov, A., Sibley, S., Thompson, M. E., & Forrest, S. R. (1998). *Nature*, *395*, 151.
[3] Friend, R. H., Gymer, R. W., Holmes, A. B., Burroughes, J. H., Marks, R. N., Taliani, C., Bradley, D. D. C., Dos Santos, D. A., Bredas, J. L., Löglund, M., & Salaneck, W. R. (1999). *Nature*, *397*, 121.
[4] Aziz, H., Popovic, Z. D., Hu, N.-X., Hor, A.-M., & Xu, G. (1999). *Science*, *283*, 1900.
[5] Baldo, M. A., Thompson, M. E., & Forrest, S. R. (2000). *Nature*, *403*, 750.
[6] Adachi, C., Baldo, M. A., Forrest, S. R., Lamansky, S., Thompson, M. E., & Wong, R. C. (2001). *Appl. Phys. Lett.*, *78*, 1622.
[7] Fukuda, Y., Watanabe, T., Wakimoto, T., Miyaguchi, S., & Tsuchida, M. (2000). *Synth. Met.*, *111–112*, 1.
[8] Holmes, R. J., Forrest, S. R., Sajoto, T., Tamayo, A., Djurovich, P. I., Thompson, M. E., Brooks, J., Tung, Y. J., D'Andrade, B. W., Weaver, M. S., Kwong, R. C., & Brown, J. J. (2005). *Appl. Phys. Lett.*, *87*, 243507.
[9] Li, G. & Shinar, J. (2003). *Appl. Phys. Lett.*, *83*, 5359.
[10] Liu, S. W., Huang, C. A., Yang, J. H., Chen, C. C., & Chang, Y. (2004). *Thin Solid Films*, *453–454*, 312.
[11] Lu, H. T., Tsou, C. C., & Yokoyama, M. (2005). *J. Crystal Growth*, *277*, 388.

[12] Zou, L., Savvate'ev, V., Booher, J., Kim, C. H., & Shinar, J. (2001). *Appl. Phys. Lett.*, *79*, 2282.
[13] Wu, C. C., Lin, Y. T., Chiang, H. H., Cho, T. Y., Chen, C. W., Wong, K. T., Liao, Y. L., Lee, G. H., & Peng, S. M. (2002). *Appl. Phys. Lett.*, *81*, 577.
[14] Im, W. B., Hwang, H. K., Lee, J. G., Han, K. J., & Kim, Y. K. (2001). *Appl. Phys. Lett.*, *79*, 1387.
[15] Chen, B., Zhang, X. H., Lin, X. Q., Kwong, H. L., Wong, N. B., Lee, C. S., Gambling, W. A., & Lee, S. T. (2001). *Syn. Met.*, *118*, 193.
[16] Huang, J., Yang, K., Xie, Z., Chen, B., Jiang, H., & Liu, S. (1998). *Appl. Phys. Lett.*, *73*, 3348.
[17] Fujita, S., Nakazawa, T., Asano, M., & Fujita, S. (2000). *Jpn. J. Appl. Phys.*, *39*, 5301.
[18] Qiu, Y., Gao, Y., Wang, L., Wei, P., Duan, L., Zhang, D., & Dong, G. (2002). *Appl. Phys. Lett.*, *81*, 3540.
[19] Choo, D. C., Yoon, Y. B., Lee, D. U., Kim, T. W., Lee, H. K., & Kim, Y. K. (2007). *Molecular Crystals and Liquid Crystals*, *470*, 269.
[20] Kim, C. H. & Shinar, J. (2002). *Appl. Phys. Lett.*, *80*, 2201.
[21] Hamada, Y., Kanno, H., Tsujioka, T., Takahashi, H., & Usuki, T. (1999). *Appl. Phys. Lett.*, *75*, 1682.
[22] Adachi, C., Baldo, M. A., & Forrest, S. R. (2000). *J. Appl. Phys.*, *87*, 8049.
[23] Hosokawa, C., Higashi, H., Nakamura, H., & Kusumoto, T. (1995). *Appl. Phys. Lett.*, *67*, 3853.
[24] Tsou, C. C., Lu, H. T., & Yokoyama, M. (2005). *J. Crystal Growth*, *280*, 201.
[25] Bang, H. S., Han, S. M., Lee, D. U., Kim, T. W., Kim, J. H., Seo, J. H., & Kim, Y. K. (2006). *IMID/IDMC'06 Digest*, 1030.